Synaptic and Neurochemical Characterization of Parallel Pathways to the Cytochrome Oxidase Blobs of Primate Visual Cortex

Y. DING[1] **AND V.A. CASAGRANDE**[1,2,3*]
[1]Department of Cell Biology, Vanderbilt University, Nashville, Tennessee 37232
[2]Department of Psychology, Vanderbilt University, Nashville, Tennessee 37232
[3]Department of Ophthalmology and Visual Sciences, Vanderbilt University, Nashville, Tennessee 37232

ABSTRACT

The primary visual cortex (V1) of primates is unique in that it is both the recipient of visual signals, arriving via parallel pathways (magnocellular [M], parvocellular [P], and koniocellular [K]) from the thalamus, and the source of several output streams to higher order visual areas. Within this scheme, output compartments of V1, such as the cytochrome oxidase-(CO) rich blobs in cortical layer III, synthesize new output pathways appropriate for the next steps in visual analysis. Our chief aim in this study was to examine and compare the synaptic arrangements and neurochemistry of elements involving direct lateral geniculate nucleus (LGN) input from the K pathway with those involving indirect LGN input from the M and P pathways arriving from cortical layer IV.

Geniculocortical K axons were labeled via iontophoretic injections of wheat germ agglutinin-horseradish peroxidase into the LGN and intracortical layer IV axons (indirect P and M pathways to the CO-blobs) were labeled by iontophoretic injections of Phaseolus vulgaris leucoagglutinin into layer IV. The neurochemical content of both pre- and postsynaptic profiles was identified by postembedding immunocytochemistry for γ-amino butyric acid (GABA) and glutamate. Sizes of pre- and postsynaptic elements were quantified by using an image analysis system, BioQuant IV.

Our chief finding is that K LGN axons and layer IV axons (indirect input from M and P pathways) exhibit different synaptic relationships to CO blob cells. Specifically, our results show that within the CO blobs: 1) all K cell axons contain glutamate, and the vast majority of layer IV axons contain glutamate with only 5% containing GABA; 2) K axons terminate mainly on dendritic spines of glutamatergic cells, while layer IV axons terminate mainly on dendritic shafts of glutamatergic cells; 3) K axons have larger boutons and contact larger postsynaptic dendrites, which suggests that they synapse closer to the cell body within the CO blobs than do layer IV axons. Taken together, these results suggest that each input pathway to the CO blobs uses a different strategy to contribute to the processing of visual information within these compartments. J. Comp. Neurol. 391:429–443, 1998. © 1998 Wiley-Liss, Inc.

Indexing terms: GABA; glutamate; immunocytochemistry; koniocellular; parvocellular; magnocellular

The primary visual cortex (V1) of primates is unique in that it is both the recipient of visual signals arriving via parallel pathways from the thalamus and the source of output streams to higher order visual areas (Casagrande, 1994; Casagrande and Kaas, 1994). Within the output layers of primate V1, visual receptive fields are physiologically distinct from their lateral geniculate nucleus (LGN) inputs (Hubel and Wiesel, 1968), suggesting that V1 may create (or synthesize) visual signals appropriate to the functional requirements of the different extrastriate visual areas. The periodic cytochrome oxidase (CO) rich compartments within primate V1, referred to most commonly as CO blobs or puffs (Hendrickson et al., 1981; Horton and

Hubel, 1981; Wong-Riley and Carroll, 1984; Wong-Riley, 1994), contain one source of output cells with physiologically distinct properties (Livingstone and Hubel, 1984; Tootell et al., 1988a,b; T'so and Gilbert, 1988; DeBruyn et al., 1993; Edwards et al., 1995; but see Leventhal et al., 1995). These metabolically active output zones are special in that they receive input from all three LGN pathways, direct input from the koniocellular (K) pathway (Casagrande and DeBruyn, 1982; Livingstone and Hubel, 1982; Fitzpatrick et al., 1983; Weber et al., 1983; Diamond et al., 1985; Lachica and Casagrande, 1992; Hendry and Yoshioka, 1994; Ding and Casagrande, 1997), and indirect input from both the magnocellular (M) and parvocellular (P) pathways (Livingstone and Hubel, 1984; Casagrande et al., 1992, Lachica et al., 1992, 1993; Boyd et al., in preparation; but see Yoshioka et al., 1994). CO blob cells project to CO thin stripes in visual area 2 (V2) as well as to other visual areas (DeYoe and Van Essen, 1985; Shipp and Zeki, 1985; Merigan and Maunsell, 1993; DeYoe et al., 1994; Shipp and Zeki, 1995). The connections of CO blobs appear to be similar across different primate species; the direct K input has been seen in all studied primates: owl monkeys (Diamond et al., 1985; Ding and Casagrande, 1997); squirrel monkeys (Fitzpatrick et al., 1983; Weber et al., 1983); macaque monkeys (Livingstone and Hubel, 1987; Hendry and Yoshioka, 1994); and bush babies (Diamond et al., 1985; Lachica and Casagrande, 1992). Although the general arrangement of connections of the V1 output compartments, such as the CO blobs, are beginning to be understood (see Casagrande and Kaas, 1994, for review), we still know little about how the three parallel input pathways are integrated within these compartments. In particular, we know next to nothing about the synaptic organization and neurochemistry of elements within the CO blobs that involve the K pathway or the indirect M and P pathways arriving from cortical layer IV. Therefore, the primary objective of this study was to examine and compare the ultrastructural relationships and transmitter content of the CO blob synaptic arrangements involving these pathways.

Previous studies of the synaptic circuitry of primate LGN input pathways have focused upon layer IV, the cortical target layer of the M and P pathways (Garey and Powell, 1971; Tigges and Tigges, 1979; Winfield and Powell, 1983; Freund et al., 1989). Within this layer, studies in macaque monkey have reported that axons from both pathways contact similar postsynaptic elements (Freund et al., 1989). Although there is some disagreement over the exact percentages, there is general agreement that the majority of M and P axons contact dendritic spines, a minority contact dendritic shafts, and very few contact somata (Tigges and Tigges, 1979; Freund et al., 1989). In cat V1, LGN afferents provide synapses to a similar variety of postsynaptic elements, spines being the major targets of both types of axons (LeVay and Gilbert, 1976; Winfield and Powell, 1976, 1983; Freund et al., 1985a,b; Einstein et al., 1987). Identified M and P axon terminal profiles in macaque monkeys are likely to contain an excitatory transmitter since they are negative for γ-amino butyric acid (GABA; Garey and Powell, 1971; Tigges and Tigges, 1979; Winfield and Powell, 1983; Freund et al., 1989). These data are reinforced by studies in rats and cats demonstrating that the terminals of geniculocortical axons are enriched with glutamate (Montero, 1990, 1994; Kharazia and Weinberg, 1994). In macaque monkeys, only a small minority of elements postsynaptic to M or P axons contain the inhibitory transmitter GABA (Freund et al., 1989). In fact, the major targets of geniculocortical afferents in layer IV of monkeys are spines of spiny stellate cells. If K axons also contact spines within the CO blobs their impact could still be different given that spiny stellate cells are missing from layer III (Lund, 1984). One would predict that if K axons contact spines they could have an important impact directly on spine bearing pyramidal output neurons. K axons might also be expected to engage in quite distinct synaptic arrangements within the CO blobs, given the differences in physiological responses between K LGN cells projecting to CO blobs vs. M and P cells projecting to layer IV (for review, see Irvin et al., 1986; Casagrande and Norton, 1991).

In light of the above, the specific aims of this study were: 1) to compare the postsynaptic elements contacted by the LGN K cell axons with those contacted by axons from cortical layer IV (indirect input from the M and P pathways) within the CO blobs; 2) to identify the neurotransmitter contents of K LGN and layer IV axons, as well as the neurotransmitter contents of their postsynaptic targets; and 3) to compare the sizes of presynaptic terminals and postsynaptic dendrites of the direct K and the indirect M and P pathways. We used the owl monkey for this study, both because its visual system is well studied (Casagrande and Kaas, 1994) and because we have detailed knowledge from our own work of the termination of K axons in cortex and the connections of layer IV with the superficial cortical layers (Casagrande et al., 1992; Ding and Casagrande, 1997; Boyd et al., unpublished observations).

MATERIALS AND METHODS

Four hemispheres from four adult owl monkeys (*Aotus trivirgatus*) were used in the present study. Two hemispheres from two animals were employed to examine synaptic arrangements of K LGN axons within the CO blobs of layer IIIB of V1. K axons were labeled via iontophoretic injections of wheat germ agglutinin conjugated to horseradish peroxidase (WGA-HRP) centered within LGN layer K3, the interlaminar cell layer between the M and P layers. Two hemispheres from the remaining two animals were used to examine the synaptic circuits within the CO blobs that involved axons from cortical layer IV, the synaptic target zone of the LGN M and P pathways. Layer IV axons were labeled via iontophoretic injections of the kidney bean lectin Phaseolus vulgaris leucoagglutinin (PHA-L). All of the monkeys were cared for according to the National Institutes of Health Guide for the Care and Use of Laboratory Animals and the guidelines of the Vanderbilt University Animal Care Committee. The nomenclature used to identify owl monkey LGN and cortical layers has been described previously (see Ding and Casagrande, 1997).

Surgical procedures

All procedures were carried out under aseptic conditions while the animals were deeply anesthetized. Prior to surgery, atropine sulfate (0.1 mg/kg) was given to inhibit salivation. The owl monkeys then were intubated, anesthetized with isofluorane (3–4%) in oxygen, and maintained with the same gas mixture at 1–2%. Heart and respiration rates were continuously monitored and reflexes tested

periodically; animals were kept warm with a water circulating heating pad throughout surgery. Once deeply anesthetized, the monkeys were secured in a stereotaxic apparatus, the skull was exposed, and a craniotomy was performed.

Labeling K LGN cell axons. A dural flap was elevated and 5% agar in saline was spread over the pial surface to prevent desiccation. For identification of K axons, evoked responses to a flashing light were recorded from the LGN through an electrode glued to a pipette (20–30 µm inner tip diameter) filled with 1% WGA-HRP in saline. When K layer 3 was identified on the basis of changes in eye dominance and relative position in the LGN, WGA-HRP was iontophoretically injected for 30 minutes (3 seconds ON/3 seconds OFF, 3–5 µA). When the injections were completed, the dural flap was repositioned, and the skin was sutured.

Labeling layer IV cell axons. For identification of cortical layer IV axons, small slits were made in the dura (1 mm apart), and a glass pipette (20 µm inner tip diameter), containing 2.5–5% PHA-L in 0.05 M phosphate buffer (pH 7.4), was lowered into V1 to depths that ranged from 450 to 700 µm. Tracers were iontophoretically injected for 5 to 10 minutes (7 seconds ON/7 seconds OFF, 1–3 µA). At the end of each injection, the pipette was left in place for 5–10 minutes, retracted, positioned at a new location (at least 1 mm away from the previous one), and another injection was made. Ten injections were made per cortical hemisphere, all restricted to the dorsal bank of primary visual cortex (V1). When the injections were completed, the skin was sutured.

Postoperatively, all animals were given 0.02 mg/kg of Banamine as an analgesic and 300,000 units/kg of a long acting penicillin (Flocillin) and monitored carefully until they were fully conscious and capable of eating and drinking on their own. At that point, they were returned to their home cages and provided with soft palatable foods and water. Details of the surgery were similar to those described earlier (Lachica and Casagrande, 1992; Lachica et al., 1993; Ding and Casagrande, 1997).

Histological procedures

After a 2-day (WGA-HRP cases) or 7- to 14-day (PHA-L cases) survival period, the animals were anesthetized deeply with an overdose of Nembutal. The animals that had received WGA-HRP injections were initially perfused transcardially with a brief rinse of oxygenated saline, then perfused with 2% paraformaldehyde/1.5% glutaraldehyde in 0.1 M phosphate buffer (pH 7.4) at 4°C. The PHA-L-injected animals were perfused the same way except that the fixative contained 2% paraformaldehyde/1.5% glutaraldehyde/0.2% picric acid in 0.1 M phosphate buffer (pH 7.4). All animals were then perfused with fixative containing 4% sucrose. The brains were removed and postfixed in 4% sucrose/fixative at 4°C for 1 hour. They were then rinsed in three changes of 0.1 M phosphate buffer (pH 7.4), and placed in 4% sucrose in the same buffer at 4°C overnight. The following day, visual cortex was blocked anterior to V2 and was dissected from the remainder of the cortical hemisphere. Then, parasagittal 60 µm sections were cut on a vibratome. In the cases that received LGN injections, the thalamus was removed and sectioned parasagittally at 52 µm on a freezing microtome.

WGA-HRP histochemistry. In the cases receiving WGA-HRP injections, all cortical and LGN sections were treated with a modified tetramethyl benzidine (TMB) and stabilization procedure (Mesulam, 1978; Horn and Hoffman, 1987). Sections were then mounted on gelatin-coated slides, air dried, dipped briefly in a clearing agent (Histo-Clear), and coverslipped. Counterstaining was unnecessary in these cases since LGN and cortical layers were clearly visible in the TMB-treated sections.

PHA-L immunocytochemistry. In the cases receiving PHA-L injections, the cortical sections were incubated for 48 hours in Tris-buffered saline (TBS) containing 2% normal rabbit serum and an antibody raised against PHA-L (Vector Labs, Burlingame, CA) at a 1:2,000 dilution. The tissue was then incubated for 2.5 hours in a linking antibody (biotinylated rabbit anti-goat) at a 1:200 dilution. Sections were then developed with diaminobenzidine (DAB) as a chromogen with 1% nickel ammonium sulfate and 0.01% hydrogen peroxide after being incubated with avidin-biotin-peroxidase complex (ABC, Vector Labs) for 2 hours. Every fourth section was also treated to show CO-blobs in cortical layer III (Wong-Riley, 1979).

EM preparation and postembedding immunocytochemistry

Tissue preparation for EM. Processed sections with well-labeled axons were treated with 1% osmium tetroxide in 0.1 M phosphate buffer at 4°C and dehydrated in graded ethanols into propylene oxide, and then infiltrated with Epon resin overnight. After polymerization at 60°C for 2 days and prior to ultrathin sectioning, CO blob tissue containing WGA-HRP labeled K axons or PHA-L labeled axons from layer IV were dissected out with a NeuroPunch (Ted Pella, Redding, CA). Since K LGN cell axons have been found to project exclusively to CO blobs in cortical layer III (Diamond et al., 1985; Ding and Casagrande, 1997), no adjacent sections were stained with CO in the cases in which K geniculocortical axons were labeled with WGA-HRP. However, for the PHA-L labeled layer IV axons, neuropunches in layer III were made only in zones aligned with a CO blob on the adjacent section. These neuropunches were centered on the CO blob within IIIB. A small portion of IIIA and IIIC was included within these punches but was later removed when the block was trimmed before ultrathin sectioning.

Postembedding immunocytochemistry for glutamate and GABA. Ultrathin silver/gold sections were cut with a diamond knife and mounted on Formvar-coated single-slot nickel grids. Modified techniques, originally described by Phend et al. (1992) to optimize post-embedding double staining for glutamate and GABA immunocytochemistry, were used in this study. Ultrathin sections were rinsed for 5 minutes in TBST (0.05 M Tris in saline and 0.1-0.2% Triton X-100, pH 7.6). The Triton was used to enhance penetration of the antibody. Sections on grids were incubated in 1:200–400 polyclonal primary anti-glutamate antibody (raised in rabbits, Chemicon International Inc., Temecula, CA) overnight. After rinsing in TBST, pH 7.6 and in TBST, pH 8.2, sections were incubated in a secondary antibody, goat anti-rabbit IgG conjugated to gold (10 nm or 15 nm in a very few cases, BioCell, distributed by Ted Pella) diluted 1:20 in TBST, pH 8.2 for 1–2 hours. After completion of the glutamate immunostaining, binding sites were deactivated over paraformaldehyde vapors in an 80°C oven for 1 hour. Sections were then incubated for 24–48 hours at a 1:200–500 dilution of a polyclonal anti-GABA (raised in rabbits, Sigma, St. Louis, MO) antibody,

followed by incubation in a goat anti-rabbit IgG conjugated to gold (20 nm, BioCell) secondary antibody, diluted 1:20–40, for 1–2 hours. The sections then were rinsed first in TBST (pH 7.6), and in deionized water, and finally were stained with uranyl acetate and lead citrate.

Controls. The specificities of anti-glutamate and anti-GABA antibodies were evaluated by preabsorbing the primary antibodies with an excess of glutamate conjugated to bovine serum albumin and/or GABA. Immuno-staining for the appropriate antibody was completely eliminated in these controls. Additional controls involved the application of rabbit pre-immune serum, as well as processing a series of immunoreactions in which various steps were omitted from the regular staining sequence. In these controls, the immunoreactivity was almost completely abolished. Controls also were done to determine denaturation of free anti-IgG binding sites for the first secondary antibody (goat anti-rabbit IgG conjugated to gold, 10 nm). The efficacy of the latter deactivation was almost 100%.

Data collection and analysis

All LGN injection sites were reconstructed from serial sections using a microprojector at low magnification (170x) to document the location and extent of the WGA-HRP label. The cortical PHA-L injections were reconstructed from serial sections through the full extent of the labeled area. Injection sites were defined as those sites containing a dark focus of label. Grids were viewed on a Hitachi H 800 electron microscope at 100 kV. Data were collected by selecting well-labeled terminals (WGA-HRP or PHA-L) with post-synaptic elements. Terminal labeling and synapse identification was confirmed by examining two or more serial sections in almost all cases. However, no effort was made to serially section every bouton to determine the exact number of synaptic contacts made by each. Pre- and postsynaptic profiles were considered immunoreactive for the neurochemical content if more than three gold particles were found over them. The average level of background labeling was extremely low (average $<$ 1 per terminal). Typically, no gold particles were observed in control sections. The maximum number of gold particles found over any elements in control sections was two. Grids with poor immunostaining were excluded from the sample. Sections were examined and photographed at 15,000x.

Measures were made of the cross-sectional areas of all labeled terminal profiles and the post-synaptic dendritic shafts in which both pre- and postsynaptic profiles were distinct and the pre-synaptic element was clearly labeled for either WGA-HRP or PHA-L. No effort was made to correct for possible differences in shrinkage between sections due to tissue processing. All measurements were made with the aid of the BioQuant-IV image analysis system (R&M Biometric Inc., Nashville, TN). Axon terminal and dendritic shaft profiles were grouped by size: small, medium, and large. Size ranges were chosen simply by dividing the total range of sizes into three equal groups, excluding the few very large outliers. For axon terminal profiles, the groups were defined as follows: small, $\leq$0.3 μm^2; medium, $>$0.3–$\leq$0.6 μm^2; and large, $>$0.6–0.9 μm^2. A very small number of larger axon terminal profiles seen were also included in the large group. For dendritic shafts, the definition of small was $\leq$0.4 μm^2; medium, $>$0.4–$\leq$0.8 μm^2; and large, $>$0.8–1.2 μm^2. A very small number of larger dendritic shafts were also included in the large group.

RESULTS

Our chief finding is that K LGN axons and layer IV axons (indirect input from M and P) exhibit different synaptic relationships to CO blob cells. Specifically, our results show that within the CO blobs: 1) K axons terminate mainly on dendritic spines of glutamatergic cells, while layer IV axons terminate mainly on dendritic shafts of glutamatergic cells; 2) K axons have larger size boutons and contact larger postsynaptic dendrites which suggest that they synapse closer to the cell body in the circuits within the CO blobs than layer IV axons; 3) all K cell axons contain glutamate, and the vast majority of layer IV axons contain glutamate with only 5% containing GABA. Each of these findings is documented in more detail below.

Injection sites and light microscopic features

Prior work has demonstrated that in owl monkey V1, M LGN axons terminate within IVα, P LGN axons in IVβ, and K axons within the CO blobs of layers III and in layer I (Kaas et al., 1976; Diamond et al., 1985; Pospichal et al., 1994). Cells located in the principal interlaminar zone between the magnocellular and parvocellular layers (layer K3) are the main K LGN cells that contribute axons to the centers of single CO blobs (Ding and Casagrande, 1997). Prior work in owl monkeys also has demonstrated that cells in both sublayers IV and IVβ (targets of the LGN M and P pathways, respectively) send axons to the CO blobs in layer III (Casagrande et al., 1992; Boyd et al., in preparation). Our aim in this study was to label LGN K3 axons through LGN injections centered in LGN K3. For comparison, we wished to label both subdivisions of cortical layer IV in order to include axons from cells targeted by both the P and M pathways without invading other cortical layers.

Figure 1A shows a darkfield photomicrograph of geniculocortical projections following an injection of WGA-HRP centered within K3 but involving the adjacent M and P LGN layers. The distinct patchy label focused within layer IIIB (see arrows in Fig. 1) arises from LGN layer K3 and this label colocalizes with the CO blobs (Ding and Casagrande, 1997). Fifteen neuropunches were made of well-labeled patches, such as the one shown in the center of Figure 1A and used for EM analysis. Figure 1B shows an example of two small injections of PHA-L (open arrows) that were made into cortical layer IV. The injections shown were both centered in the top of IVβ (P target) but also involved IVα (M target). The injections shown result in axonal label (see arrow in Fig. 1B) within the CO blobs as determined on adjacent sections. Other injections (not shown) were centered either in the middle of layer IV or within IVα or IVβ. A total of six injections, all on the dorsal bank of V1, were selected based upon the criteria that they involved both subdivisions of layer IV, were restricted to layer IV, and exhibited well-labeled axons within the CO blobs.

K pathway synaptic arrangements

A total of 130 WGA-HRP labeled K axon terminal profiles were identified by the presence of electron-dense reaction product (Figs. 2–4). These geniculocortical terminals are loosely packed with clear round vesicles, the majority containing one to several mitochondria. These identified K geniculate terminals are exclusively presynaptic and usually form single, asymmetric synaptic contacts with dendritic profiles, both spines and shafts. In the
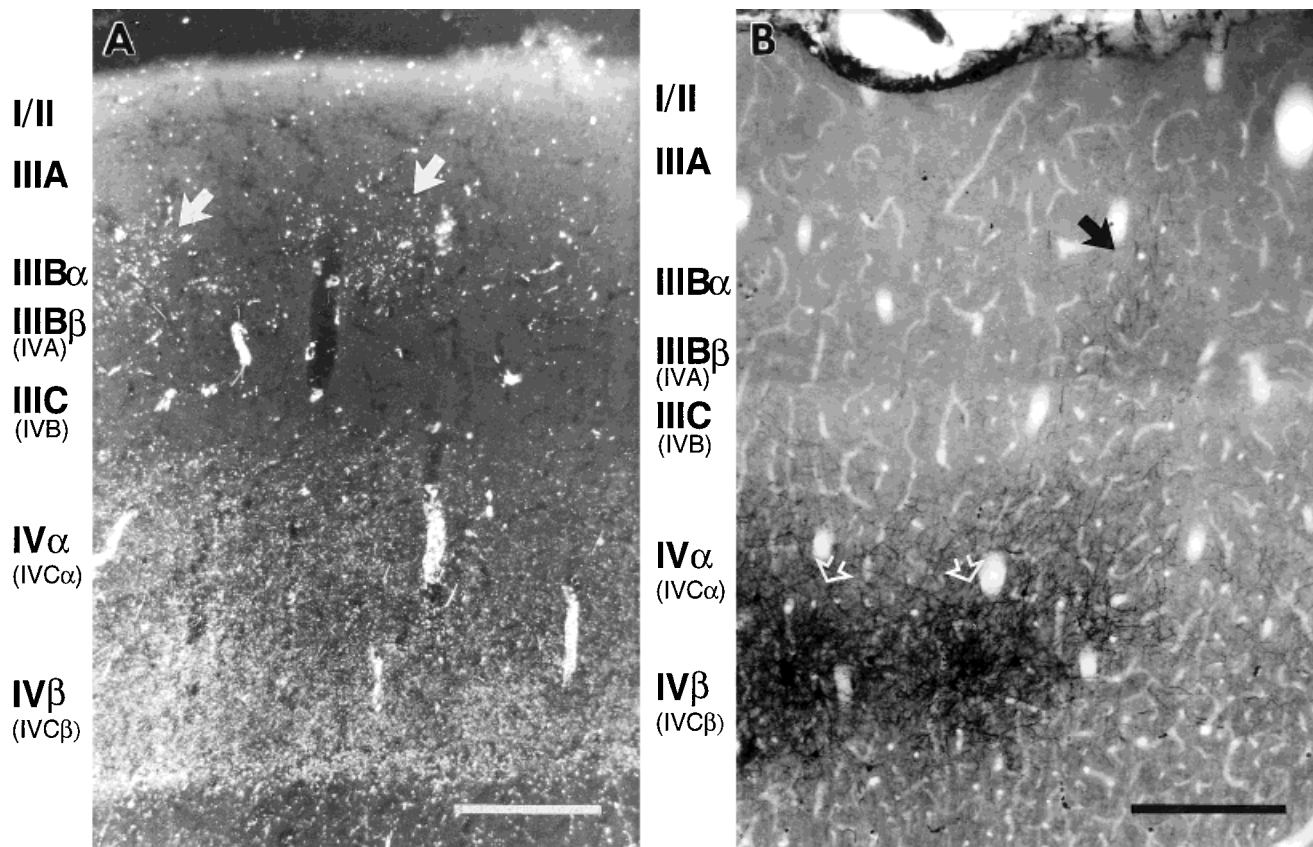
Fig. 1. **A**: A darkfield photomicrograph of geniculocortical projections following an injection of wheat germ agglutinin-horseradish peroxidase (WGA-HRP) centered within koniocellular (K) layer 3 but involving the adjacent magnocellular (M) and parvocellular (P) lateral geniculate nucleus (LGN) layers. The distinct patchy label focused within layer IIIB (indicated by arrows) arises from LGN layer K3. **B**: An example of two small injections of Phaseolus vulgaris leucoagglutinin (PHA-L; indicated by open arrows) that were made into cortical layer IV. The injections shown were both centered in the top of IVβ (P target) but also involved IVα (M target). The injections shown result in axonal label (indicated by an arrow) within the cytochrome oxidase-(CO) blobs of IIIBα, as determined on adjacent sections. Roman numerals refer to the cortical layers. We use a modification of the nomenclature originally proposed by Hässler (1967). Brodmann's (1909) laminar designations are given in parentheses (if different). Scale bars = 0.5 mm.

present study, we use the criteria proposed originally by Freund et al. (1989) to distinguish dendritic spines from shafts. According to these criteria, all dendritic profiles that contain mitochondria and/or microtubules are classified as dendritic shafts regardless of their diameter, and all small dendrites lacking mitochondria and microtubules are classified as dendritic spines. As described by Freund et al. (1989) for macaque monkeys, in owl monkeys some dendritic profiles classified as dendritic shafts, because of their mitochondrial or microtubular content, are similar in shape, and as small in size, as profiles classified as spines.

Using these criteria, we determined that 61% of K axons terminate on dendritic spines (see Fig. 2) and 39% terminate on dendritic shafts (see Figs. 3, 4). Labeled K axons do not appear to synapse with cell bodies or other axons. In general, K axons tend to be involved in simple synaptic relationships with either one dendritic spine or one dendritic shaft. All of the dendritic spines receiving synaptic input from a labeled K terminal appear to get exclusive input from that terminal. However, a number of larger dendritic shafts (glutamatergic or GABAergic) that receive synaptic input from K axons also receive input from a GABAergic axon (Fig. 4A) as well as asymmetric synapses from other axonal sources (Figs. 3A,B, 4B). Additionally,

4% of K axons make contact with two postsynaptic profiles, two spines (Fig. 2D) or one spine and one shaft (Fig. 3C). A few K axons also exhibit perforated synapses (Nieto-Sampedro et al., 1982) with dendritic shafts. These percentages are likely to be an underestimate since serial reconstructions through the entire bouton were not performed.

All of the WGA-HRP-labeled K terminal profiles contain a number of small gold particles (10 nm; see Figs. 2–4; examples are indicated by outline arrows) suggesting that they are immunoreactive for glutamate; none of these terminals are immunoreactive for GABA (identified by larger 20 nm gold particles; [see Figs. 2A, 4]; examples are indicated by outline arrowheads). The majority (90%) of the postsynaptic dendritic spines also are immunoreactive for glutamate (see Figs. 2A–C, 3C). The remainder of the spines contain no label. Sixty-eight percent of dendritic shafts contacted by K terminals are immunoreactive for glutamate (Fig. 3), 26% are immunoreactive for GABA (Fig. 4), and the remaining 6% are unlabeled.

Synaptic arrangements of layer IV axons

A total of 178 terminals were identified as PHA-L labeled axons from layer IV based upon electron dense
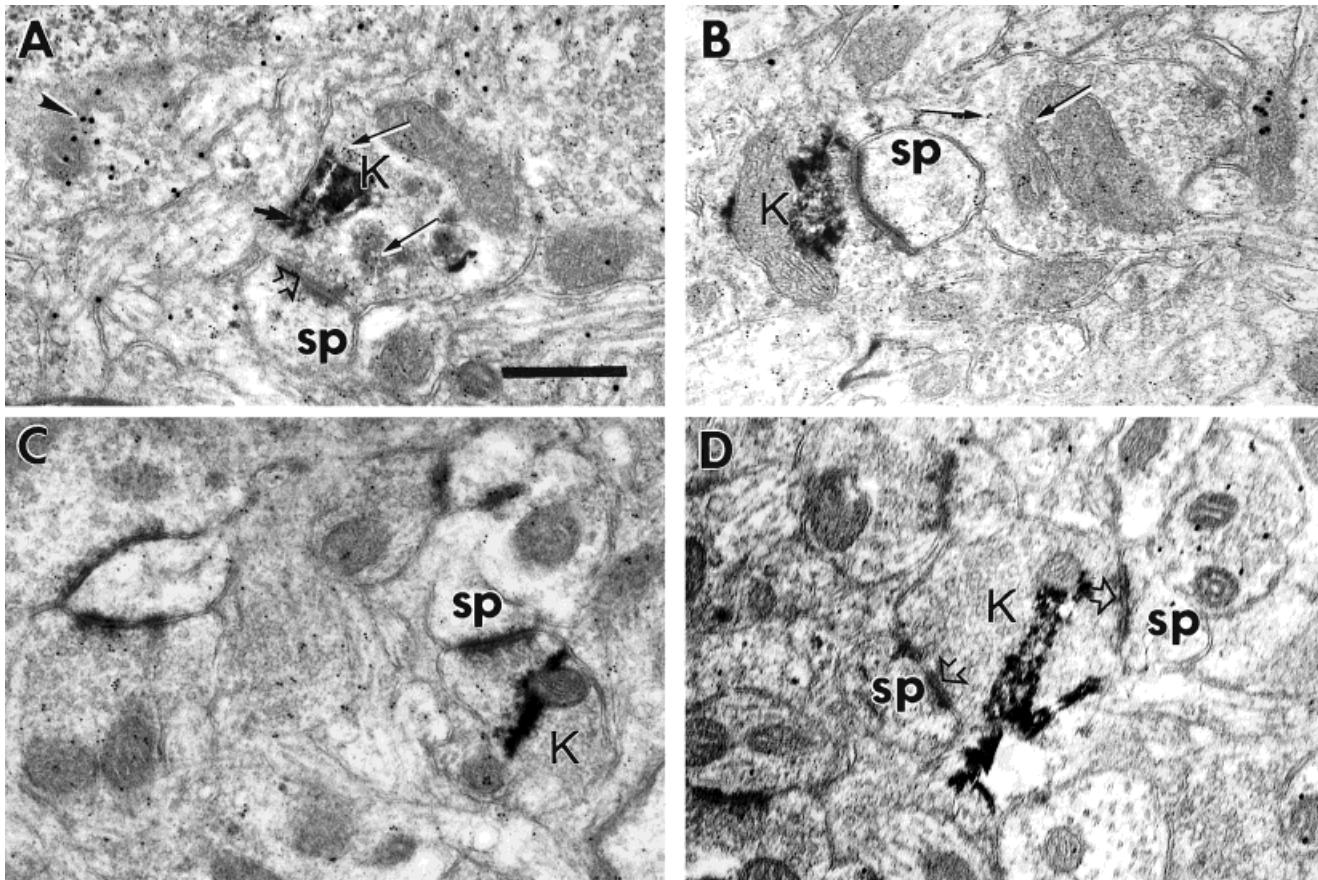
Fig. 2.   WGA-HRP labeled K axon terminals (indicated by K) were identified by electron-dense reaction product (an example is indicated by a filled arrow in A), and they make asymmetric synapses (examples are indicated by open arrows) on spines (indicated by sp; **A–C)**. K axons use glutamate (small black dots; examples are indicated by outline arrows in A and B) and end on glutamatergic dendritic spines. Larger gold particles (20 nm) showing immunoreactivity for γ-amino butyric acid (GABA) are seen as larger black dots (an example is indicated by outline arrowhead in A). K axons occasionally make synapses (open arrows) with two postsynaptic spines **(D)**. Scale bar = 0.5 μm.

reaction product (Figs. 5–7). Layer IV axon terminals, unlike K axons, are characterized by tightly packed round vesicles, and the majority contain at most one mitochondrion. Where clear synaptic contacts are observed between labeled layer IV axons and postsynaptic elements, the vast majority (95%) are asymmetric. Examples of darkly labeled layer IV axons synapsing on a dendritic spine are shown in Figure 5. Labeled axon terminal profiles from layer IV are presynaptic, exclusively forming single synaptic contacts with dendritic profiles; no multiple contacts were seen. However, complete serial sections of these small, darkly-labeled boutons would be required to be certain that multiple contacts do not exist. It is also rare to find elements postsynaptic to layer IV axons receiving other contacts. Only two examples of the latter were seen, one in which a labeled and unlabeled bouton made asymmetric synapses with the same spine (not shown), and one in which a labeled and two unlabeled boutons made asymmetric synapses with the same dendritic shaft (Fig. 6C). Unlike K axons, the minority (42%) of layer IV axons within the CO-blobs terminate on dendritic spines (see Fig. 5), and the majority (57%) terminate on dendritic shafts (see Fig. 6). Two examples of layer IV axons terminating on glutamatergic cell bodies also were seen (see Fig. 7A).

The vast majority (95%) of axons from layer IV contain a number of small gold particles indicative of immunoreactivity for glutamate (Figs. 5–7). Only 5% of layer IV axons are positive for GABA, indicated by the presence of large gold particles (20 nm, Fig. 7B). Seventy percent of spines postsynaptic to layer IV axons are immunoreactive for glutamate (Fig. 5), 3% of spines are positive for GABA, and the remainder are unlabeled. The majority (74%) of dendritic shafts receiving contacts from labeled layer IV axons also contain glutamate (Fig. 6A–C). Twenty percent of postsynaptic dendritic shafts contain a number of larger gold particles indicative of immunoreactivity for GABA (Fig. 6D). The remainder of the postsynaptic shafts were unlabeled.

Quantitative comparisons

In order to provide a more detailed comparison of K and layer IV axons within the CO-blobs, we examined the area of all presynaptic profiles. Figure 8A shows the percentage of terminal profiles that fall into three size categories. Only 20% of K axons have small terminals ($\leq$0.3 μm^2 in area) compared with the vast majority (80%) of layer IV axon terminal profiles that fall in this size category. The majority (54%) of K axons end as medium sized terminals ($>$0.3–$\leq$0.6 μm^2 in area), while only 18% of layer IV presynaptic terminals fall in this size category. Twenty-six
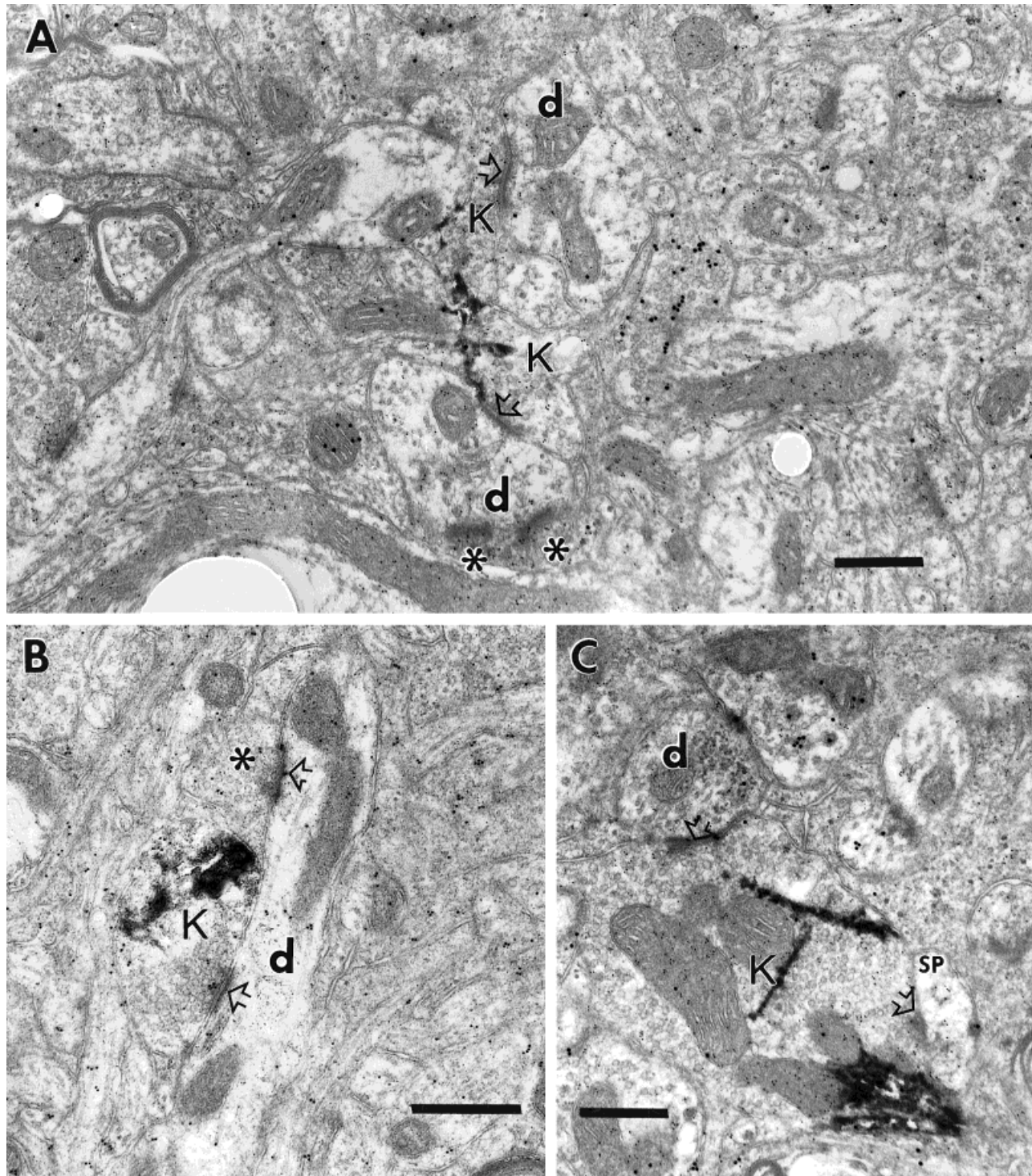
Fig. 3. K axons contacting glutamatergic dendritic shafts (indicated by d). Larger dendritic shafts can receive synaptic input from a K axon as well as input from other glutamatergic axonal sources (indicated by asterisks; **A,B**). K axons can make contact with two postsynaptic profiles, in this case, one spine and one shaft **(C).** Other conventions are as in Figure 2. Scale bars = 0.5 μm.

percent of all K axons have large terminals ($>$0.6 μm² in area), compared to only 2% of layer IV terminals. On average, presynaptic K axon terminal areas ($\bar{x}$ = 0.52 $\pm$ 0.36 μm², n = 130) are significantly larger than layer IV axon terminal areas ($\bar{x}$ = 0.23 $\pm$ 0.11 μm², n = 178).

A similar comparison was made between the sizes of postsynaptic dendrites contacted by K versus layer IV axons. Here we restricted the comparison to dendritic shafts. As shown in Figure 8B, K axons tend to make contact with larger dendritic shafts than layer IV axons.
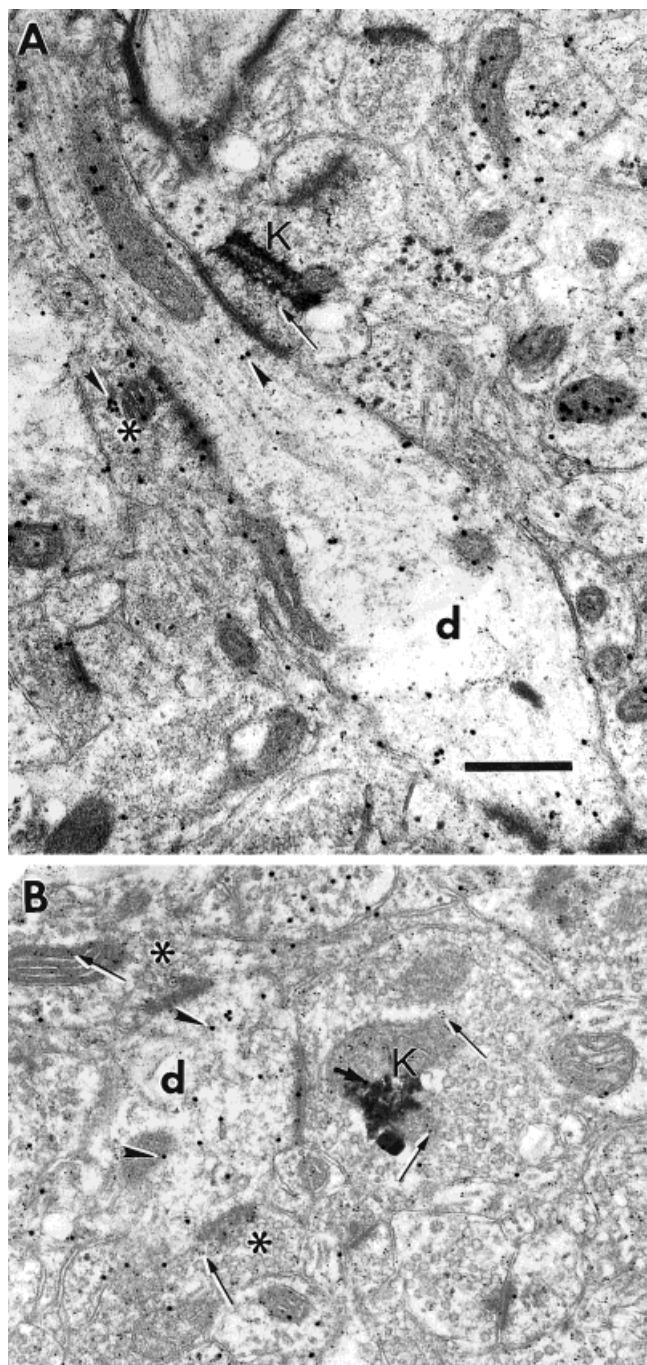
Fig. 4.   Some K axons synapse on inhibitory GABAergic (identified by large gold particles) dendritic shafts. The larger dendritic shafts receiving synaptic input from K axons also receive input from GABAergic **(A)** or glutamatergic axons **(B)**; indicated by asterisks. Other conventions are as in Figure 2. Scale bar = 0.5 μm.

The majority (56%) of layer IV axons terminate on small (≤0.4 μm² in area) dendritic shafts, whereas only a minority (33%) of K axons terminate on dendritic shafts in this size range. The majority (44%) of K axons and 37% of layer IV axons contact medium (≤0.8 μm² in area) dendritic shafts. Twenty-three percent of the K axons synapse on large (>0.8 μm² in area) dendritic shafts, compared to

only 7% of layer IV axons. These data suggest that some K axons may have a larger impact on cell responses than axons carrying P and M signals from layer IV since the former could synapse closer to the cell body/axon hillock assuming that they influence the same cells.

DISCUSSION

Our chief aim in this study was to examine and characterize the arrangements and neurochemistry of synapses in CO blobs made both by direct LGN input from the K pathway and indirect LGN input from the M and P pathways arriving from cortical layer IV. Our findings show that all K axons and the vast majority of layer IV axons within the CO blobs contain glutamate. The bulk of these axons also terminate upon dendrites that contain glutamate. However, several aspects of the synaptic arrangements and relative sizes of terminal boutons and postsynaptic profiles suggest that, although they share some features in common, each pathway uses a different strategy to contribute to the processing of visual information within the CO blobs. Figure 9 summarizes these features.

In the following sections, we first compare the synaptic arrangements made by K LGN axons in layer III with reported arrangements made by M and P LGN axons in layer IV. Next, we contrast the synaptic circuits in the CO blobs that involve layer IV axons with those involving K axons. Finally, we consider the functional implications of our findings.

Synaptic arrangements made by LGN axons

Our data show that the K geniculocortical axons in owl monkey layer III engage in similar synaptic arrangements to those reported for M and P geniculocortical axons in layer IV of the macaque monkey (Garey and Powell, 1971; Winfield et al., 1982; Freund et al., 1989). At present, there are no data on the synaptic arrangements made by P and M axons in owl monkeys although the light microscopic structure and distribution of these axons in layer IV is analogous to what has been described in other primates, including macaque monkeys (Kaas et al., 1976; Diamond et al., 1985; Pospichal et al., 1994). Our results show that presynaptic owl monkey K profiles in the CO blobs are consistently immuno-positive for glutamate and make asymmetric (Gray's type I) synapses; no K axon terminal profiles are found to be immuno-positive for GABA. Within macaque monkey layer IV, M and P axons also have been reported to make asymmetric synapses, hinting that they too contain the excitatory transmitter glutamate (Garey and Powell, 1971; Winfield et al., 1982; Freund et al., 1989). Although direct immunocytochemical confirmation of the presence of glutamate has not been reported for primate M and P axon terminals in layer IV, the proposal that these axons use glutamate is reinforced by a number of studies demonstrating that geniculate relay cells or geniculo-cortical axons in other mammals contain glutamate (Montero, 1990, 1994; Kharazia and Weinberg, 1994).

K axons in owl monkey layer III and M and P axons in layer IV in other primates contact similar postsynaptic elements. For all three pathways, the most common target is the dendritic spine. Our results show that 61% of K axons contact spines. In macaque monkey, Freund et al. (1989) reported, using the same criteria for spine identification, that 52–69% of M and P axons also contact spines
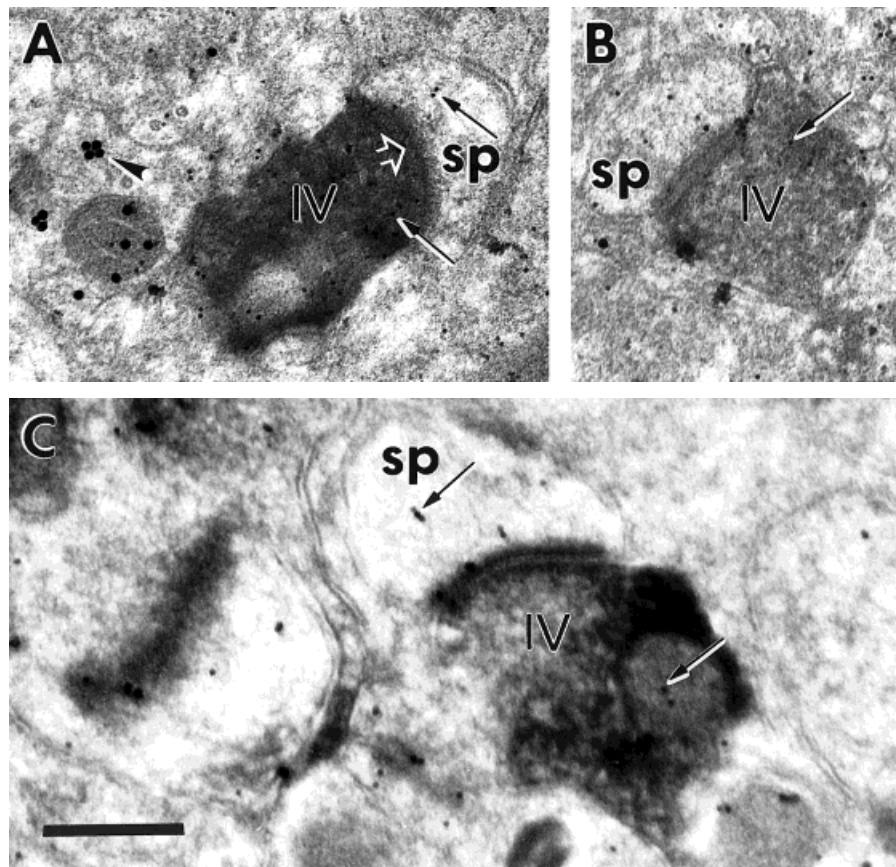
Fig. 5. PHA-L-labeled layer IV axon terminals (indicated by IV) are identified by dark electron-dense reaction product that generally fills the entire terminal **(A–C).** The majority of layer IV (indirect M and P) axons use glutamate and a minority of them end on glutamatergic dendritic spines. Other conventions are as in Figure 2. Scale bar = 0.3 µm.

in layer IV. The higher percentages of M and P contacts with spines in layer IV (up to 90%) reported by others for macaque and squirrel monkey (Garey and Powell, 1971; Tigges and Tigges, 1979; Winfield et al., 1982; Winfield and Powell, 1983) likely reflect a more liberal criteria for defining a spine. Given that most spine bearing cells are reported to contain an excitatory transmitter (Greenamyre and Porter, 1994; Nieuwenhuys, 1994), it is not surprising that we find that the majority (90%) of spines postsynaptic to K axons are immuno-positive for glutamate with the remainder immuno-negative; none are immuno-positive for GABA. Since both glutamate and aspartate have been reported to be released in the visual cortex during activation of visual pathways (Tamura et al., 1990), it is possible that the profiles postsynaptic to K axons that are negative for glutamate and GABA use aspartate as a neurotransmitter. In layer IV of macaque monkeys, spines postsynaptic to M and P axons are also exclusively immuno-negative for GABA (Freund et al., 1989) or have been directly identified as belonging to presumed excitatory spiny stellate neurons (Garey and Powell, 1971; Winfield et al., 1982). In addition to spines, owl monkey K boutons contact dendritic shafts, of which the majority (68%) use glutamate with 26% containing GABA and 6% remaining immuno-negative for both. Again, since both glutamate and aspartate have been reported to be released in the visual cortex during activation of visual

pathways, it is possible that the dendritic shafts postsynaptic to K axons that are negative for glutamate and GABA use aspartate as a neurotransmitter. Therefore, 74% of dendritic shafts are presumed to be excitatory. Taken together, 90% of the entire population of the profiles (spines and shafts) postsynaptic to K axons are excitatory and the remaining 10% are immuno-positive for GABA. M and P boutons in layer IV of macaque monkey also contact dendritic shafts, 80% of which are presumed to be excitatory based upon immunonegativity for GABA. Consequently, about 90% of postsynaptic elements were identified as excitatory in macaque monkey (Freund et al., 1989). The tendency for geniculocortical axons to contact predominantly spines of excitatory cells, and to a lesser extent dendritic shafts of excitatory cells, extends also to both cat X and Y geniculo-cortical boutons in area 17 and cat Y axons in area 18, as well as to rat geniculocortical axons in area 17 (Garey and Powell, 1971; LeVay and Gilbert, 1976; Winfield and Powell, 1976; Peters and Feldman, 1977; Winfield and Powell, 1983; Freund et al., 1985a; Kharazia and Weinberg, 1994), suggesting that these are general features of the geniculocortical axons in mammals.

In spite of the above similarities, we know that the physiology of different geniculocortical pathways and their target cells are distinct (Casagrande and Norton, 1991; Merigan and Maunsell, 1993). Therefore, one might expect to see some of these distinctions reflected at the ultrastruc-
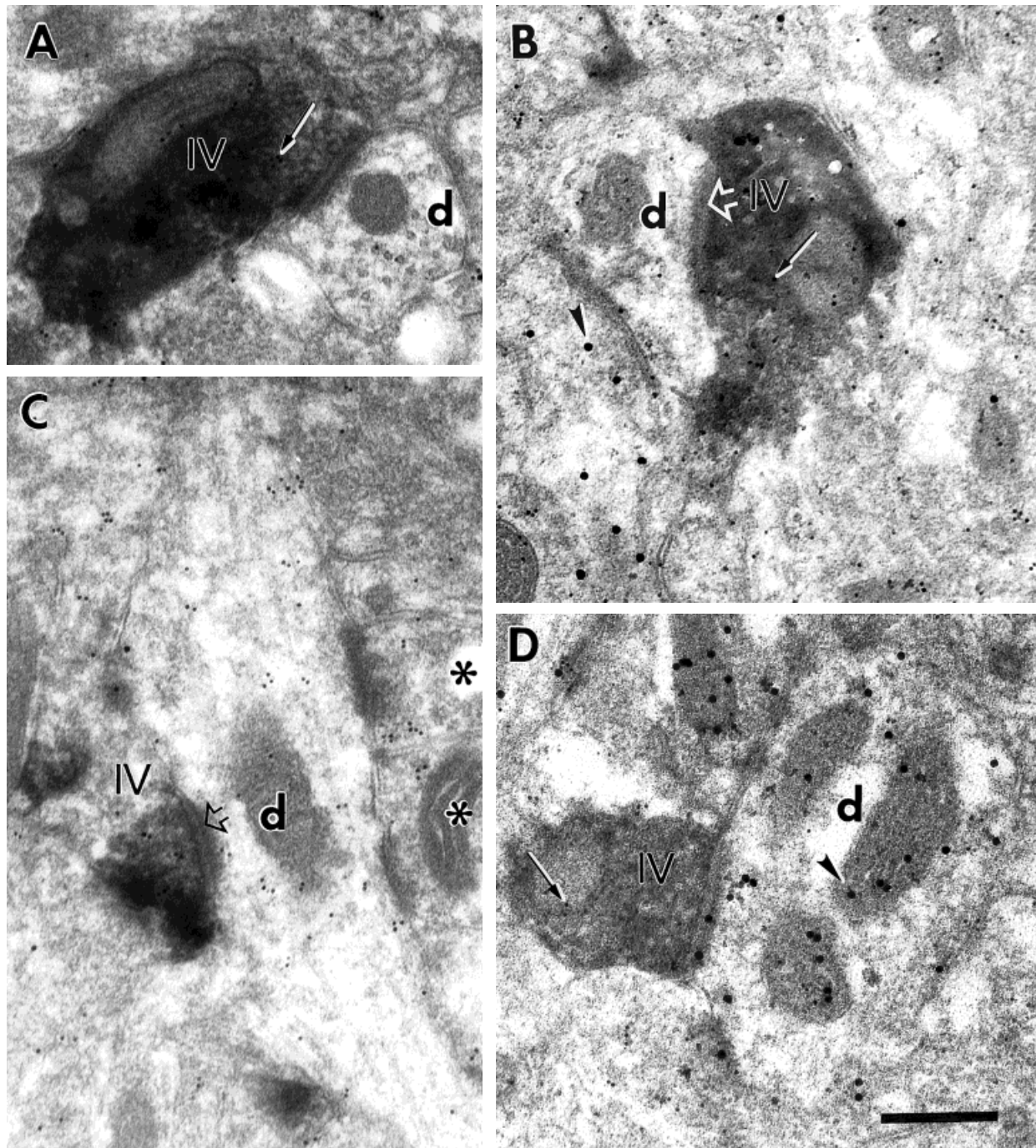
Fig. 6. The majority of layer IV (indirect M and P) axons contact glutamatergic dendritic shafts **(A–C).** A significant minority of layer IV axons synapse on inhibitory GABAergic dendritic shafts **(D)**. C shows a larger dendritic shaft (glutamatergic) receiving synaptic input from a layer IV axon as well as other glutamatergic axonal sources (indicated by asterisks). Other conventions are as in Figure 2. Scale bar = 0.3 μm.

tural level in cortex. A difference between the circuits involving K axons in layer III and the circuits involving M and P axons in layer IV (again comparing between primate species) concerns the relative number of synaptic contacts made per bouton. The vast majority of owl monkey K boutons make single synaptic contacts with postsynaptic profiles. Only 4% make contact with two postsynaptic profiles, in this instance two spines, or one spine and one shaft. In macaque monkeys and squirrel monkeys, a significant percentage of both P and M axons have been reported to make more than one synapse. In studies of single sections (comparable to this study) 15% of P axons and 24% of M axons in macaque monkeys were found to make multiple synaptic contacts (Winfield et al., 1982). In
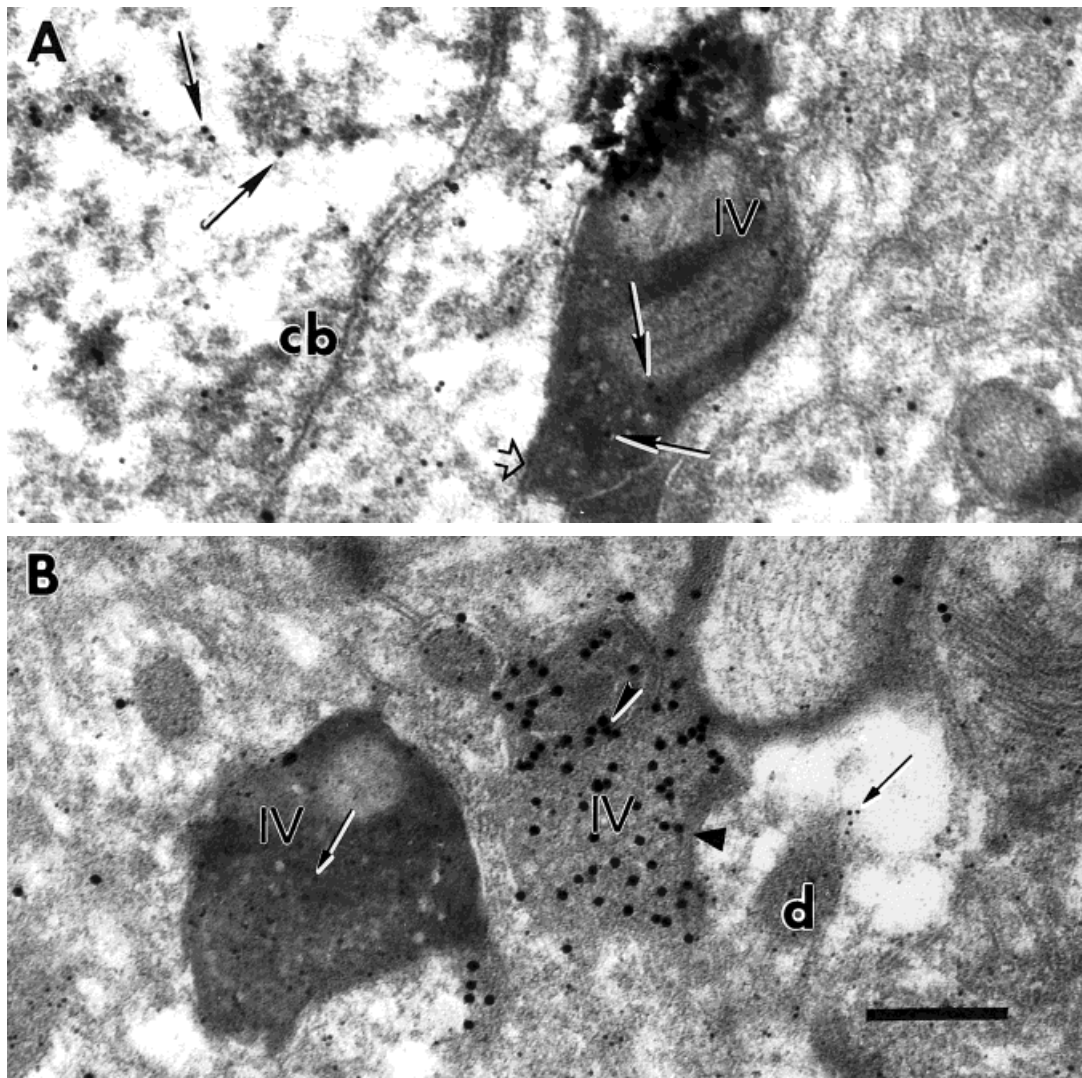
Fig. 7. **A**: A very small number of layer IV axons (glutamatergic, indicated by 15 nm gold particles; examples are indicated by outline arrows) also terminate on glutamatergic cell bodies (indicated by cb). **B**: Only 5% of layer IV axons are positive for GABA, identified by the presence of large gold particles (20 nm gold particles) within the terminal. This terminal is synapsing (arrowhead) on a glutamatergic dendritic shaft (indicated by smaller, 10 nm, gold particles). Other conventions are as in Figure 2. Scale bar = 0.3 µm.

serial sections, the same investigators report that these percentages rose to 27% and 82%, respectively. Number of synaptic contacts has been correlated to bouton size, with the larger M boutons making more synaptic contacts than the smaller P boutons. Serial reconstructions would be required to provide a more precise estimate of the number of multiple contacts made by individual K boutons. We also would need comparable data for M and P boutons in owl monkeys to make appropriate comparisons. However, based strictly upon a comparison of single section EM data across species and LM bouton size within the owl monkey (Pospichal et al., 1994 and unpublished observations), one would predict that owl monkey K boutons make fewer multiple contacts than either M or P boutons.

Additionally, types of axon and dendritic interactions that are possible within the CO blobs compared to layer IV are different. The blobs receive numerous intrinsic and a greater variety of extrinsic connections than have been reported in layer IV. In addition to axons from cells in both IV and IVβ (the M and P recipient sublayers), CO blobs in owl monkeys (the subjects of this study) have been reported to receive input from cells in all cortical layers except layer I, as well as input from local cells (Casagrande et al., 1992, Boyd et al., in preparation). Extrinsic connections of the CO blobs include not only the LGN K pathway, but also a number of extrastriate visual areas (especially feedback from V2), as well as input from the pulvinar (Casagrande and Kaas, 1994). As in layer IV, the major neuropil component of the CO blobs consists of dendrites. However, there is a very important difference. Within the CO blobs there are no spiny stellate cells (Lund, 1984). Therefore in the CO blobs, all dendritic spines arise from either local pyramidal cells or pyramidal cells from other layers, especially layer V (Peters and Sethares, 1991). By this arrangement, K axons have direct access to output neurons, unlike the axons of M and P cells which are said
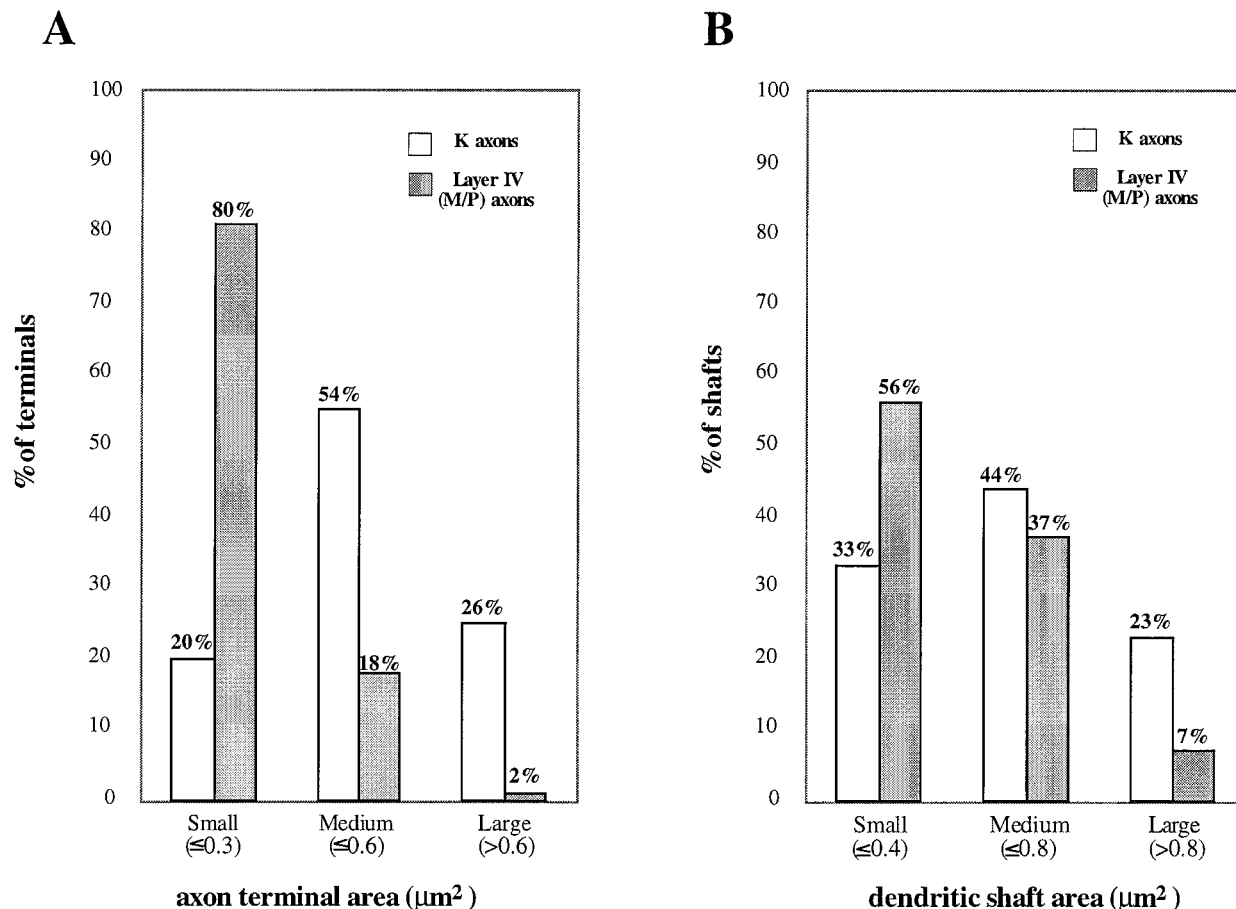
A

B

Fig. 8. **A**: The size distributions of K and layer IV (indirect M and P) axon terminals in the CO blobs. K axons range in size from 0.3 μm² or less (small) to greater than 0.6 μm² (large) but on average are medium (0.3–0.6 μm²) in size. Layer IV axons exhibit the same size range but the vast majority (80%) are small, 0.3 μm² or less. **B**: The size distributions of postsynaptic dendritic shafts. K axons contact mainly medium (0.4–0.8 μm², in area) dendritic shafts, whereas layer IV axons contact mainly small (≤0.4 μm², in area) dendritic shafts. Twenty-three percent of the K axons appear to synapse on large (>0.8 μm², in area) dendritic shafts, compared to only 7% of layer IV axons.

to avoid pyramidal cell apical and basal dendrites and terminate exclusively on spiny stellate cells (Lund, 1984). Taken together, these data could either suggest that K axons are more powerful in producing an effect on the output of V1, because they could contact output cells directly, or are less powerful because they are outside the amplification that the circuitry of spiny stellate cells affords the M and P axons.

CO blob synaptic circuits

Comparison of K, M, and P axon circuits, as described above, shows that, with the exception of some differences in the number of multiple contacts, these circuits are surprisingly similar. However, relative to the CO blob output cells of V1, the impact of each of these pathways may be quite different, since K axons terminate directly in the blobs and M and P signals reach the blobs after first passing at least one synapse in layer IV. A comparison of layer IV boutons and K boutons within the CO blobs shows that there are several differences which could be functionally significant. Unlike K boutons, the majority (61%) of which terminate on dendritic spines, the majority (57%) of layer IV boutons terminate on dendritic shafts. Layer IV boutons are smaller in size and contact smaller dendritic

shafts, on average, than do K boutons and never appear to make multiple synaptic contacts. Additionally, unlike K axons, a small number (1%) of layer IV boutons are found to contact somata. The net effect of these differences in wiring between the two pathways entering the CO blobs is a matter of speculation (see also below), but must be considered in the context of what is known about the local circuitry within this region.

As mentioned above, in the owl monkey as in other primates, the CO blobs are not only targets of axons from the K pathway and layer IV, but also axons from other cortical layers such as IIIBβ, IIIC, and V within the same column, as well as axons from pyramidal cells in other CO blobs and feedback connections from higher order visual cortical areas (see Casagrande and Kaas, 1994 for review). Although we have not performed a detailed analysis of the synaptic neuropil in the CO blobs in owl monkeys, Wong-Riley and colleagues have examined the cell types and synaptic circuitry of macaque monkey CO blobs in some detail (Nie and Wong-Riley, 1995). In macaque monkeys, the CO blob neuropil is complex and consists of dendrites from a variety of pyramidal and non-pyramidal cells. These investigators report that 72% of synapses in macaque CO blobs are asymmetrical and mainly occur on
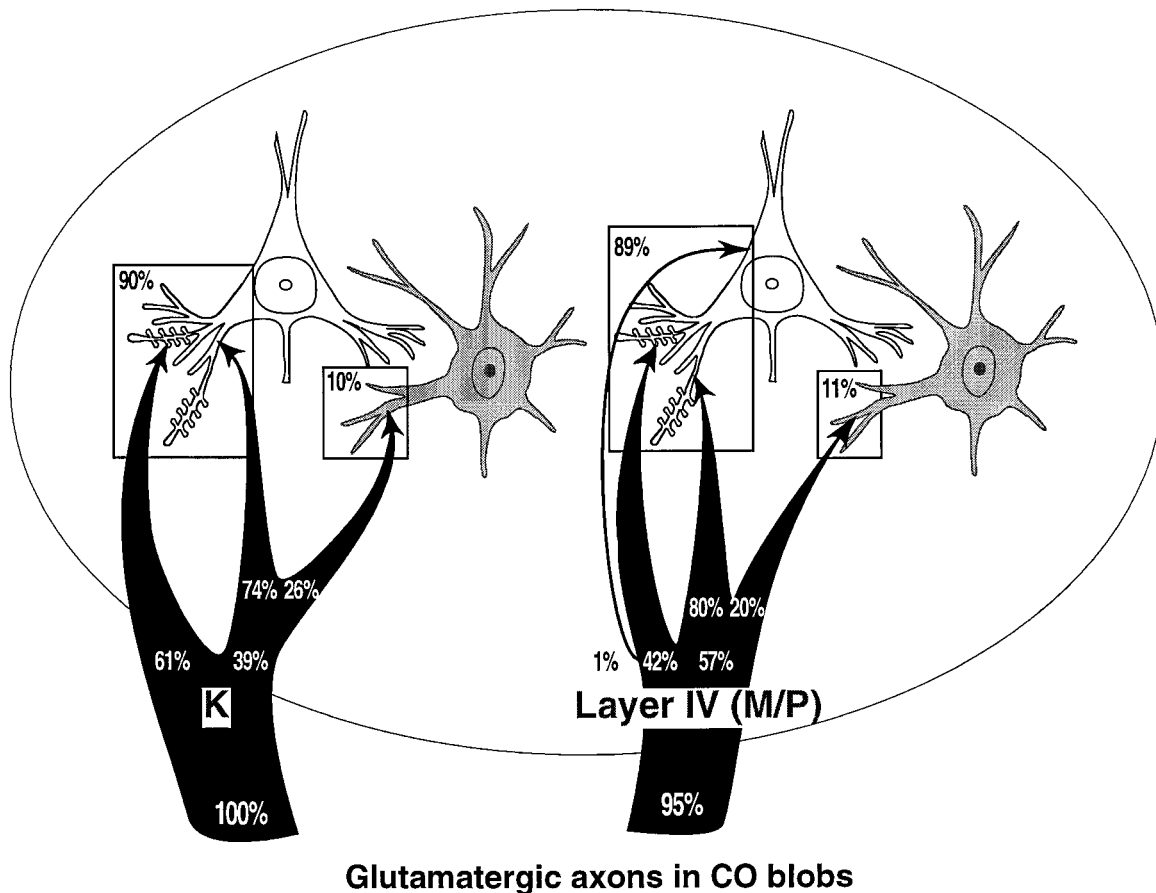
Glutamatergic axons in CO blobs

Fig. 9. A schematic diagram summarizing the inputs from the different visual pathways to the CO-blob in the cortical layer III. The two cell types, pyramidal neuron (open) and interneuron (filled) are shown. All K axons use glutamate as a neurotransmitter. Sixty-one percent of K axons terminate on dendritic spines, which were identified as excitatory. The remaining K axons terminate on dendritic shafts, of which 74% are excitatory and 26% contain the inhibitory transmitter, GABA. Thus, 90% of K axons terminate on excitatory with only 10% terminating on interneurons. Ninety-five percent of layer IV (M/P pathway) axons use glutamate as a neurotransmitter and 5% use GABA (not shown in the figure). In contrast to K axons, axons from layer IV terminate mainly (57%) on dendritic shafts, 80% of which are identified as excitatory; the remaining 20% contain GABA. Only 42% of layer IV axons terminate on dendritic spines, most of which were identified as excitatory. One percent of layer IV axons also contact somata, which appear to be positive for glutamate. Taken together, 89% of layer IV axons terminate on excitatory neurons, with the remaining 11% terminating on interneurons.

dendritic spines, although some contact dendritic shafts, and, more rarely, the somata of GABAergic interneurons. The remaining 28% of synapses in the blobs are symmetrical and occur on dendritic shafts, and more rarely on somata of GABAergic interneurons. Beaulieu et al. (1992) also reported that within the CO blobs, 20% of the total number of cortical neurons and 17% of the synapses are GABAergic. The major targets of GABAergic synapses are dendritic shafts, comprising nearly two-thirds of the postsynaptic elements. About two-thirds of non-GABAergic synapses are on dendritic spines. Within this context, it is interesting that K axons follow the norm of local synapses which are found mostly on spines, whereas the boutons arriving from layer IV end more often on dendritic shafts. However, without knowledge of the relationship of other axonal sources to dendritic spines and shafts, it is difficult to know how these differences translate into function.

Functional implications

The receptive field properties of CO blob cells have not been examined in the owl monkey. A number of studies have found physiological differences between CO blob and interblob compartments in macaque monkeys (Livingstone and Hubel, 1984; Tootell et al., 1988a,b; T'so and Gilbert, 1988; Edwards et al., 1995). Current dogma emphasizes that the properties of CO blob and interblob compartments are specialized to relay information about color and form, respectively, to area V2 (Hubel, 1988; Zeki, 1993). Since owl monkeys are nocturnal and have only one cone type (Wikler and Rakic, 1990; Kemp and Jacobson, 1991; Jacobs et al., 1993), it seems unlikely that the CO blobs are specialized to convey chromatic information in this species. Nevertheless, even in the bush baby, another nocturnal primate with only one cone type (Deegan and Jacobs, 1996), CO blobs and interblobs show differences in receptive field properties indicative of functional specialization (DeBruyn et al., 1993). Additionally, the projections of CO blob and interblob compartments to extrastriate areas in all primates are distinct from each other but similar across species. Taken together, these data suggest that CO blob compartments perform some

special visual function that transcends species differences (Casagrande and Kaas, 1994).

At present, we still know so little about the synaptic circuitry of different compartments and layers in V1 that it is impossible to relate physiological data to synaptic circuitry except in very rare circumstances. Our data do provide evidence that K LGN axons within the CO blobs share more in common with other LGN axons terminating within layer IV than they do with axons projecting from layer IV to the CO blobs. Our data also reinforce previous LM data showing that layer IV cells project directly to the CO blobs (Casagrande et al., 1992; Lachica et al., 1992, Lachica et al., 1993; Boyd et al., in preparation). Thus, it seems reasonable that all three LGN pathways are integrated within these compartments, although it is still possible that they terminate on different classes of cells. It is noteworthy that in our material the number of labeled K or layer IV profiles encountered per 100 μm^2 was quite low especially for the labeled K axons. If this is a true reflection of the density of these projections and not a technical artifact, then it would suggest that neither K axons nor axons from layer IV make up more than a small percentage of the synapses within each individual blob. Although physiological evidence has indicated that thalamic input plays an essential role in driving cortical cells in layer IV (Malpeli et al., 1981, 1986; Tanaka, 1983; Malpeli, 1983; Ferster et al., 1996), geniculocortical afferent terminals represent less than 20% of the asymmetrical synapses in layer IV (Garey and Powell, 1971; Tigges and Tigges, 1979; Peters et al., 1994) and a very small proportion in layer III (the present study, as mentioned above). The majority of the intrinsic circuits within layer III are also excitatory, accounting for 75–85% of the total synaptic connections that any single neuron in V1 receives (Beaulieu et al., 1992). These data indicate that activity in the CO blobs arriving through each of the LGN pathways is integrated with the activity from a series of other layer-specific cortical connections. Clearly, further studies are needed. In particular, it will be important to determine if K axons and layer IV axons terminate on the same cell and whether these cells represent an intrinsic population or are output cells to extrastriate areas. Additionally, it will be important to understand if different pathways to the same compartment utilize the same or different glutamate receptors. Together with the current findings, such data should help us appreciate how specific synaptic circuits might translate into functional specialization within the output pathways to extrastriate cortex.

ACKNOWLEDGMENTS

LITERATURE CITED

Beaulieu, C., Z. Kisvarday, P. Somogyi, M. Cynader, and A. Cowey (1992) Quantitative distribution of GABA-immuno-positive and -immuno-negative neurons and synapses in the monkey striate cortex (area 17). Cerebral Cortex *2:*295–309.

Brodmann, K. (1909) Vergleichende Lokalisationlehre der Grosshirnrinde in ihren Prinzipien dargestellt auf Grund des Zellenbaues. J.A. Barth, Leipzig.

Casagrande, V.A. (1994) A third parallel visual pathway to primate area V1. Trends in Neuroscience *17:*305–310.

Casagrande, V.A., and E.J. DeBruyn (1982) The galago visual system: Aspects of normal organization and developmental plasticity. In D.E. Haines (ed): The Lesser Bush Baby (Galago), An Animal Model: Selected Topics. Boca Raton, Florida: CRC Press, pp. 138–162.

Casagrande, V.A., and J.H. Kaas (1994) The afferent, intrinsic, and efferent connections of primary visual cortex in primates. In A. Peters and K.S. Rockland(eds): Cerebral Cortex. New York: Plenum Press, pp. 201–259.

Casagrande, V.A., J.A. Mavity-Hudson, and J.G. Taylor (1992) Intrinsic connections of owl monkey cortex: Difference between cytochrome oxidase (CO) blobs and interblobs. Soc. Neurosci. Abstr. *18:*389.

Casagrande, V.A., and T.T. Norton (1991) Lateral geniculate nucleus: A review of its physiology and function. In A.G. Leventhal (ed): The Neural Basis of Visual Function. London: The Macmillan Press, pp. 41–84.

DeBruyn, E.J., V.A. Casagrande, P.D. Beck, and A.B. Bonds (1993) Visual resolution and sensitivity of single cells in the primary visual cortex (V1) of a nocturnal primate (bush baby): Correlation with cortical layers and cytochrome oxidase patterns. J. Neurophysiol. *69:*3–18.

Deegan, II, J.F., and G.H. Jacobs (1996) Spectral sensitivity and photopigments of a nocturnal prosimian, the bushbaby *(Otolemur crassicaudatus)*. Am. J. Promatol. *40:*55–66.

DeYoe, E.A., D.J. Felleman, D.C. Van Essen, and E. McClendon (1994) Multiple processing streams in occipitotemporal visual cortex. Nature *371:*151–154.

DeYoe, E.A., and D.C. Van Essen (1985) Segregation of efferent connections and receptive field properties in visual area V2 of the macaque. Nature *317:*5861.

Diamond, I.T., M. Conley, K. Itoh, and D. Fitzpatrick (1985) Laminar organization of geniculocortical projections in *Galago senegalensis* and *Aotus trivirgatus*. J. Comp. Neurol. *242:*584–610.

Ding, Y., and V.A. Casagrande (1997) The distribution and morphology of LGN K pathway axons within the layers and CO blobs of owl monkey V1. Visual Neurosci. *14:*691–704.

Edwards, D.P., K.P. Purpura, and E. Kaplan (1995) Contrast sensitivity and spatial frequency responses of primate cortical neurons in and around the cytochrome oxidase blobs. Vision Res. *35:*1501–1523.

Einstein, G., T.L. Davis, and P. Sterling (1987) Ultrastructure of synapses from the A-laminae of the lateral geniculate nucleus in layer IV of the cat striate cortex. J. Comp. Neurol. *260:*63–75.

Ferster, D., S. Chung, and H. Wheat (1996) Orientation selectivity of thalamic input to simple cells of cat visual cortex. Nature *380:*249–252.

Fitzpatrick, D., K. Itoh, and I.T. Diamond (1983) The laminar organization of the lateral geniculate body and the striate cortex in the squirrel monkey (*Saimiri sciureus*). J. Neurosci. *3:*673–702.

Freund, T.F., K.A.C. Martin, I. Soltesz, P. Somogyi, and D. Whitteridge (1989) Arborization pattern and postsynaptic targets of physiologically identified thalamocortical afferents in striate cortex of the macaque monkey. J. Comp. Neurol. *289:*315–336.

Freund, T.F., K.A.C. Martin, P. Somogyi, and D. Whitteridge (1985a) Innervation of cat visual areas 17 and 18 by physiologically identified X- and Y-type thalamic afferents. II. Identification of postsynaptic targets by GABA immunocytochemistry and Golgi impregnation. J. Comp. Neurol. *242:*275–291.

Freund, T.F., K.A.C. Martin, and D. Whitteridge (1985b) Innervation of cat visual areas 17 and 18 by physiologically identified X- and Y-type thalamic afferents. I. Arborization patterns and quantitative distribution of postsynaptic elements. J. Comp. Neurol. *242:*263–274.

Garey, L.J., and T.P.S. Powell (1971) An experimental study of the termination of the lateral genico-cortical pathway in the cat and monkey. Proc Royal Soc. London, Series B *179:*41–63.

Greenamyre, J.T., and R.H. Porter (1994) Anatomy and physiology of glutamate in the CNS. Neurology *44:*S7–13.

Guillery, R.W. (1969) The organization of synaptic interconnections in the laminae of the dorsal lateral geniculate nucleus of the cat. Z. Zellforsch *96:*1–38.

Hässler, R. (1967) Comparative anatomy of the central visual systems in day- and night-active primates. In R. Hässler and H. Stephen (eds): Evolution of the Forebrain. New York: Plenum Press, pp. 419–434.

Hendrickson, A.E., S.P. Hunt, and J.-Y. Wu (1981) Immunocytochemical localization of glutamic acid decarboxylase in monkey striate cortex. Nature *292:*3–5.

Hendry, S.H.C., and T. Yoshioka (1994) A neurochemically distinct third channel in the macaque dorsal lateral geniculate nucleus. Science *264:*575–577.

Horn, A.K.E., and K.-P. Hoffmann (1987) Combined GABA-immunocytochemistry and TMB-HRP histochemistry of pretectal nuclei projecting to the inferior olive in rats, cats and monkeys. Brain Res. *409:*133–138.

Horton, J.C., and D.H. Hubel (1981) Regular patchy distribution of cytochrome oxidase staining in primary visual cortex of macaque monkey. Nature *292:*762–764.

Hubel, D.H., and T.N. Wiesel (1968) Receptive fields and functional architecture of monkey striate cortex. J. Physiol. *195:*215–243.

Hubel, D.H. (1988) Eye, brain, and vision. New York: W.H. Freeman and Company.

Irvin, G.E., V.A. Casagrande, and T.T. Norton (1993) Center/surround relationships of magnocellular, parvocellular, and koniocellular relay cells in primate lateral geniculate nucleus. Visual Neurosci. *10:*363–373.

Irvin, G.E., T.T. Norton, M.A. Sesma, and V.A. Casagrande (1986) W-like response properties of interlaminar zone cells in the lateral geniculate nucleus of a primate (*Galago crassicaudatus*). Brain Res. *362:*254–270.

Jacobs, G.H., J.F. Deegan, J. Neitz, M.A. Crognale, and M. Neitz (1993) Photopigments and color vision in the nocturnal monkey, Aotus. Vision Res. *33:*1773–1783.

Kaas, J.H., C.-S. Lin, and V. Casagrande (1976) The relay of ipsilateral and contralateral retinal input from the lateral geniculate nucleus to striate cortex in the owl monkey: A transneuronal transport study. Brain Res. *106:*371–378.

Kemp, C.M., and S.G. Jacobson (1991) The distribution and kinetics of visual pigments in the owl monkey retina. Exp. Eye Res. *52:*329–335.

Kharazia, V.N., and R.J. Weinberg (1994) Glutamate in thalamic fibers terminating in layer IV of primary sensory cortex. J. Neurosci. *14:*6021–6032.

Lachica, E.A., P.D. Beck, and V.A. Casagrande (1992) Parallel pathways in macaque monkey striate cortex: Anatomically defined columns in layer III. Proc. Natl. Acad. Sci. USA *89:*3566–3570.

Lachica, E.A., P.D. Beck, and V.A. Casagrande (1993) Intrinsic connections of Layer-III of striate cortex in squirrel monkey and bush baby - correlations with patterns of cytochrome oxidase. J. Comp. Neurol. *329:*163–187.

Lachica, E.A., and V.A. Casagrande (1992) Direct W-like geniculate projections to the cytochrome oxidase (CO) blobs in primate visual cortex-axon morphology. J. Comp. Neurol. *319:*141–158.

Lennie, P., J. Krauskopf, and G. Sclar (1990) Chromatic mechanisms in striate cortex of macaque. J. Neurosci. *10:*649–669.

LeVay, S., and C.D. Gilbert (1976) Laminar patterns of geniculocortical projection in the cat. Brain Res. *113:*1–19.

Leventhal, A.G., K.G. Thompson, D. Liu, Y. Zhou, and S.J. Ault (1995) Concomitant sensitivity to orientation, direction, and color of cells in layers 2, 3, and 4 of monkey striate cortex. J. Neurosci. *3:*1808–1818.

Livingstone, M.S., and D.H. Hubel (1984) Anatomy and physiology of a color system in the primate visual cortex. J. Neurosci. *4:*309–356.

Livingstone, M.S., and D.H. Hubel (1982) Thalamic inputs to cytochrome oxidase rich regions in monkey visual cortex. Proc. Natl. Acad. Sci. USA *79:*6098–6101.

Lund, J.S. (1984) Spiny stellate cells. In A. Peter and E.G. Jones (eds): Cerebral cortex, Vol. 1, Cellular Components of the Cerebral Cortex. New York: Plenum, pp. 255–308.

Malpeli, J.G. (1983) Activity of cells in area 17 of the cat in absence of input from layer A of lateral geniculate nucleus. J. Neurophysiol. *49:*595–610.

Malpeli, J.G., C. Lee, H.D. Schwark, and T.G. Weyand (1986) Cat Area 17. I. Pattern of thalamic control of cortical layers. J. Neurophysiol. *56:*1062–1073.

Malpeli, J.G., P.H. Schiller, and C.L. Colby (1981) Response properties of single cells in monkey striate cortex during reversible inactivation of individual lateral geniculate laminae. J. Neurophysiol. *46:*1102–1119.

Merigan, W.H., and J.H.R. Maunsell (1993) How parallel are the primate visual pathways? Ann. Rev. Neurosci. *16:*369–402.

Mesulam, M.-M. (1978) Tetramethyl benzidine for horseradish peroxidase neurohistochemistry: A non-carcinogenic blue reaction-product with superior sensitivity for visualizing neural afferents and efferents. J. Histochem. Cytochem. *26:*106–117.

Montero, V.M. (1990) Quantitative immunogold analysis reveals high glutamate levels in synaptic terminals of retino-geniculate, cortico-geniculate, and geniculo-cortical axons in the cat. Visual Neurosci. *4:*437–443.

Montero, V.M. (1994) Quantitative immunogold evidence for enrichment of glutamate but not aspartate in synaptic terminals of retino-geniculate, geniculo-cortical, and cortico-geniculate axons in the cat. Visual Neurosci. *11:*675–681.

Nie, F., and M.T. Wong-Riley (1995) Differential glutamatergic innervation in cytochrome oxidase-rich and -poor regions of the macaque striate cortex: quantitative EM analysis of neurons and neuropil. J. Comp. Neurol. *369:*571–590.

Nieto-Sampedro, M., S.F. Hoff, and C.W. Cotman (1982) Perforated postsynaptic densities: Probable intermediates in synapse turnover. Proc. Natl. Acad. Sci. USA *79:*5718–5722.

Nieuwenhuys, R. (1994) The neocortex. An overview of its evolutionary development, structural organization and synaptology. Anat. Embryol. *190:*307–337.

Norton, T.T., and Casagrande, V. A. (1982) Laminar organization of receptive-field properties in lateral geniculate nucleus of bush baby (*Galago crassicaudatus*). J. Neurophysiol. *47:*715–741.

Peters, A., and M.L. Feldman (1977) The projection of the lateral geniculate nucleus to area 17 of the rat cerebral cortex. IV. Terminations upon spiny dendrites. J. Neurocytol. *6:*669–689.

Peters, A., and C. Sethares (1991) Organization of pyramidal neurons in area 17 of monkey visual cortex. J. Comp. Neurol. *306:*1–23.

Phend, K.D., R.J. Weinberg, and A. Rustioni (1992) Techniques to optimize post-embedding single and double staining for amino acid neurotransmitters. J. Histochem. Cytochem. *40:*1011–1020.

Pospichal, M.W., S.L. Florence, and J.H. Kaas (1994) The postnatal development of geniculocortical axon arbors in owl monkeys. Visual Neurosci. *11:*71–90.

Shipp, S., and S. Zeki (1985) Segregation of pathways leading from area V2 to areas V4 and V5 of macaque monkey visual cortex. Nature *315:*322–325.

Shipp, S., and S. Zeki (1995) Segregation and convergence of specialized pathways in macaque monkey visual cortex. J. Anat. *187:*547–562.

Tamura, H., T.P. Hicks, Y. Hata, T. Tsumoto, and A. Yamatodani (1990) Release of glutamate and aspartate from the visual cortex of the cat following activation of afferent pathways. Exp. Brain Res. *80:*447–455.

Tanaka, K. (1983) Cross-correlation analysis of geniculo-striate neuronal relationships in cats. J. Neurophysiol. *49:*1303–1318.

Tigges, M., and J. Tigges (1979) Types of degenerating geniculocortical axon terminals and their contribution to layer IV in the squirrel monkey (*Saimiri*). Cell Tissue Res. *196:*4711–4786.

Tootell, R.B.H., M.S. Silverman, S.L. Hamilton, R.L. De Valois, and E. Switkes (1988a) Functional anatomy of macaque striate cortex. III. Color. J. Neurosci. *8:*1569–1593.

Tootell, R.B.H., M.S. Silverman, S.L. Hamilton, E. Switkes, and R.L. De Valois (1988b) Functional anatomy of macaque striate cortex. V. Spatial frequency. J. Neurosci. *8:*1610–1624.

T'so, D.Y., and C.D. Gilbert (1988) The organization of chromatic and spatial interactions in the primate striate cortex. J. Neurosci. *8:*1712–1727.

Weber, J.T., M.F. Heurta, J.H. Kaas, and J.K. Harting (1983) The projections of the lateral geniculate nucleus of the squirrel monkey: Studies of the interlaminar zones and the S layers. J. Comp. Neurol. *213:*113–145.

Wikler, K.C., and P. Rakic (1990) Distribution of photoreceptor subtypes in the retina of diurnal and nocturnal primates. J. Neurosci. *10:*3390–3401.

Winfield, D.A., and T.P.S. Powell (1976) The termination of thalamo-cortical fibres in the visual cortex of the cat. J. Neurocytol. *5:*269–281.

Winfield, D.A., and T.P.S. Powell (1983) Laminar cell counts and geniculo-cortical boutons in area 17 of cat and monkey. Brain Res. *277:*223–229.

Winfield, D.A., M. Rivera-Dominguez, and T.P.S. Powell (1982) The termination of geniculocortical fibres in area 17 of the visual cortex in the macaque monkey. Brain Res. *231:*19–32.

Wong-Riley, M. (1979) Changes in the visual system of monocularly sutured or enucleated cats demonstrable with cytochrome oxidase histochemistry. Brain Res. *171:*11–28.

Wong-Riley, M., and E.W. Carroll (1984) Effects of impulse blockade on cytochrome oxidase activity in monkey visual cortex. Nature *307:*262–264.

Wong-Riley, M.T.T. (1994) Primate visual cortex: Dynamic metabolic organization and plasticity revealed by cytochrome oxidase. In A. Peters and K.S. Rockland (eds): Cerebral Cortex. New York: Plenum Press, pp. 141–200.

Yoshioka, T., J.B. Levitt, and J.S. Lund (1994) Independence and merger of thalamocortical channels within macaque monkey primary visual cortex: Anatomy of interlaminar projections. Visual Neurosci. *11:*467–489.

Zeki, S. (1993) A Vision of the Brain. Boston: Blackwell Scientific Publications.